

Article

Study on the Activity Model of PbO-ZnO-FeO-Fe₂O₃-SiO₂-CaO Six-Component High-Lead Slag System

Jinbo Song [†], Wenlong Xi [†] and Liping Niu ^{*}

School of Metallurgy, Northeastern University, Shenyang 110819, China

^{*} Correspondence: niulp@smm.neu.edu.cn[†] These authors contributed equally to this work.

Abstract: In this paper, the thermodynamic properties of the PbO-ZnO-FeO-Fe₂O₃-SiO₂-CaO six-component slag system were studied by using the molecular-ion coexistence theory, and the influence of slag composition changes on the activity of each structural unit was analyzed. The results show that the calculated value of the activity model is in good agreement with the measured value of the experiment, and the activity of each structural unit is greatly affected by the composition of the slag, but less affected by the temperature. High temperature is conducive to the decomposition of lead silicate and the formation of calcium-containing compounds, but the activity of ZnO will decrease. When the mass fraction of PbO increases, the main reaction is to combine with PbO·SiO₂ to form 2PbO·SiO₂. Increasing the mass fraction of ZnO and CaO is beneficial to the decomposition of lead silicate and an increase in PbO activity. When the iron-silicon ratio increases, it will promote the decomposition of lead silicate and the formation of ZnO·Fe₂O₃, so the activity of PbO will increase and the activity of ZnO will decrease. When the calcium-silicon ratio is low, the binary combination product of CaO and SiO₂ is mainly CaO·SiO₂, and when the calcium-silicon ratio rises above 0.5, the activities of 2CaO·SiO₂ and 3CaO·2SiO₂ will increase rapidly.

Keywords: high-lead slag; molecular-ion coexistence theory; activity; thermodynamic model



Citation: Song, J.; Xi, W.; Niu, L. Study on the Activity Model of PbO-ZnO-FeO-Fe₂O₃-SiO₂-CaO Six-Component High-Lead Slag System. *Metals* **2023**, *13*, 734. <https://doi.org/10.3390/met13040734>

Academic Editor: Ricardo J. Alves de Sousa

Received: 3 March 2023

Revised: 30 March 2023

Accepted: 4 April 2023

Published: 9 April 2023



Copyright: © 2023 by the authors. Licensee MDPI, Basel, Switzerland. This article is an open access article distributed under the terms and conditions of the Creative Commons Attribution (CC BY) license (<https://creativecommons.org/licenses/by/4.0/>).

1. Introduction

Because lead-based solid waste has the characteristics of scattered sources, miscellaneous mineral phases, and is low grade and polymetallic, there are still many problems in the treatment, and an energy-saving and environmentally friendly treatment system has not been designed [1,2]. One of the current solutions is the co-smelting of lead-based solid waste and primary ore. Its advantages are mainly manifested in the following aspects. First of all, one of the common characteristics of lead-based solid waste is that there are no self-heating materials, and most of them are mainly metal oxides and sulfates. If they are treated separately, more energy will be consumed. The primary ore lead smelting is autothermal smelting, which relies on the oxidation reaction of sulfide and low-priced iron compounds to provide heat; the lead-based solid waste and primary ore are smelted together, and the heat released during primary ore smelting can be used as solid waste. Melting provides energy, which has a good effect on energy saving. Secondly, many elements in the lead-based solid waste can complement the elements in the primary ore to complete the slagging reaction during smelting, which can reduce the amount of auxiliary materials added in the smelting of the primary ore and can also play a role in saving resources. Therefore, primary ore collaborative lead-based solid waste smelting has obvious advantages in hazardous waste treatment, energy and resource conservation, etc., and the development of primary ore collaborative lead-based solid waste green smelting technology will help solve the environmental problems and problems caused by lead-based solid waste stockpiling. It is of great significance to promote the effective utilization of secondary resources.

A large number of studies by metallurgical workers have shown that there are many components and complex structures in the slag of the pyrometallurgical process. The

activity of each component in the slag largely determines the reaction that occurs in the pyrometallurgical process and has a significant impact on the phase composition of the slag. The research methods of activity mainly include the electromotive force method [3], the slag-gas equilibrium experiment method [4,5], etc. In addition, some scholars use theoretical models to predict the activity of melts, mainly including molecular structure theory [6,7], ionic structure theory [8], ion-molecule coexistence theory [9], polyelectron theory [10], etc. Although some scholars at home and abroad have conducted relevant phase equilibrium and activity studies on smelting slag systems containing PbO [11,12], there are few thermodynamic studies on primary ore collaborative lead-based solid waste smelting. Due to the shortcomings of high-temperature experimental measurement, such as complex operation, low precision, and high cost, it is very necessary to study the thermodynamic properties of high-temperature melts theoretically.

Among the many theoretical models of slag activity, the most widely used is the ion-molecule coexistence theory (IMCT). The prototype of this theory is the "Slag Ion Theory Considering Undecomposed Compounds" proposed by a professor from the former Soviet Union. Based on this theory, Professor Zhang Jian of Beijing University of Science and Technology conducted further analysis, induction, and demonstration of the activity model, and renamed it the "Slag Structure Coexistence Theory" [13–15]. The molecular-ion coexistence theory is considered to be able to better reflect the structure of the slag. The mass action concentration calculated by this theoretical model can be approximately regarded as the activity of each structural unit in the slag.

In this paper, combined with the high-temperature phase diagram of the binary slag system and the ternary slag system in the PbO-ZnO-FeO-Fe₂O₃-SiO₂-CaO six-component slag system, the structural units existing in the slag are determined, and the sum of the action concentrations of all components is stipulated to be equal to 1. Based on the principle of mass conservation of each component of the slag, a component action concentration (activity) model was established to analyze the influence of the slag composition changes on the activity of each structural unit.

2. Activity Model Building

2.1. Assumptions for Thermodynamic Models

The molecular-ion coexistence theory replaces the traditional activity with the ion pair or molecular mass action concentration in the slag, which is used to characterize the reactivity of each component and simplifies the complex situation in the slag. That is, the mass action concentration of structural units such as ion pairs or molecules in the PbO-ZnO-FeO-Fe₂O₃-SiO₂-CaO slag system can characterize its reaction ability just like the activity in the traditional sense. In order to establish a general thermodynamic model of the mass action concentration (activity) of each structural unit in the PbO-ZnO-FeO-Fe₂O₃-SiO₂-CaO slag system, it is necessary to make the following basic assumptions about the properties of the slag:

- (1) The slag is composed of simple ions (Pb²⁺, Zn²⁺, Fe²⁺, Ca²⁺, O²⁻, etc.) and simple molecules such as SiO₂ and Fe₂O₃, as well as complex molecules such as silicates and ferrites. The structural units are independent and synergistic;
- (2) The coexistence of ions and molecules is continuous throughout the composition range;
- (3) Simple structural units and complex structural units can be transformed into each other and are in dynamic equilibrium;
- (4) The form that should be taken when expressing the activity of MeO is: $a_{MeO} = N_{MeO} = N_{Me^{2+}} + N_{O^{2-}}$
- (5) The chemical reactions involving all ion pairs and molecules in the slag should obey the law of mass action.

These assumptions establish the relationship between the number of moles of the basic components in the slag and the mass action concentration of each structural unit, and link the mass action concentrations of the basic components and complex molecules to the chemical reaction equilibrium constants.

2.2. The Mass Action Concentration of Each Structural Unit

According to the IMCT theory, there are five simple ions of Pb^{2+} , Zn^{2+} , Fe^{2+} , Ca^{2+} , and O^{2-} , and two simple molecules of SiO_2 and Fe_2O_3 in the $\text{PbO-ZnO-FeO-Fe}_2\text{O}_3\text{-SiO}_2\text{-CaO}$ slag system. Meanwhile, according to the phase diagrams of PbO-SiO_2 , CaO-SiO_2 , $\text{FeO-SiO}_2\text{-CaO}$, $\text{FeO-Fe}_2\text{O}_3\text{-CaO}$, and $\text{ZnO-Fe}_2\text{O}_3\text{-SiO}_2$, in the temperature range of 1373 K~1573 K, the $\text{PbO-ZnO-FeO-Fe}_2\text{O}_3\text{-SiO}_2\text{-CaO}$ slag may form 16 kinds of composite molecules, and its structural units are listed in Table 1.

Table 1. Structural unit of the $\text{PbO-ZnO-FeO-Fe}_2\text{O}_3\text{-SiO}_2\text{-CaO}$ slag system.

Slag	Simple Ions and Molecules	Complex Molecule	Ref.
PbO-SiO_2	Pb^{2+} , O^{2-} , SiO_2	PbSiO_3 , Pb_2SiO_4 , Pb_4SiO_6	[16]
CaO-SiO_2	Ca^{2+} , O^{2-} , SiO_2	CaSiO_3 , Ca_2SiO_4 , Ca_3SiO_5 , $\text{Ca}_3\text{Si}_2\text{O}_7$,	[17]
$\text{FeO-SiO}_2\text{-CaO}$	Fe^{2+} , Ca^{2+} , O^{2-} , SiO_2	$\text{Ca}_2\text{Fe}_2\text{O}_5$, CaFe_2O_4 , CaFe_3O_5 , Fe_3O_4	[17]
$\text{FeO-Fe}_2\text{O}_3\text{-CaO}$	Fe^{2+} , Ca^{2+} , O^{2-} , Fe_2O_3	Fe_3O_4 , $\text{Ca}_2\text{Fe}_2\text{O}_5$ CaFe_2O_4 , CaFe_3O_5	[17]
$\text{ZnO-Fe}_2\text{O}_3\text{-SiO}_2$	Zn^{2+} , O^{2-} , Fe_2O_3 , SiO_2	ZnSiO_3 , Zn_2SiO_4 , ZnFe_2O_4	[17]

The mass action concentrations of the 22 ion pairs and molecules in Table 1 are N_1 , N_2 , $N_3 \dots N_{22}$ respectively. According to the definition of mass action concentrations, the formula for calculating N_i is shown in Formula (1). The molar numbers and mass action concentrations are listed in Table 2.

$$N_i = \frac{x_i}{\sum x} \quad (1)$$

Table 2. Molarity and mass action concentration of each structural unit in the slag.

Structural Unit Type	Structural Unit	Structural Unit Mole Number	Structural Unit Mass Action Concentration
simple ion pair	$(\text{Pb}^{2+} + \text{O}^{2-})$	x_1	$N_1 = 2x_1/\sum x$
	$(\text{Zn}^{2+} + \text{O}^{2-})$	x_2	$N_2 = 2x_2/\sum x$
	$(\text{Fe}^{2+} + \text{O}^{2-})$	x_3	$N_3 = 2x_3/\sum x$
	$(\text{Ca}^{2+} + \text{O}^{2-})$	x_4	$N_4 = 2x_4/\sum x$
simple molecule	SiO_2	x_5	$N_5 = x_5/\sum x$
	Fe_2O_3	x_6	$N_6 = x_6/\sum x$
complex molecule	Fe_3O_4	x_7	$N_7 = x_7/\sum x$
	$\text{CaO}\cdot\text{SiO}_2$	x_8	$N_8 = x_8/\sum x$
	$2\text{CaO}\cdot\text{SiO}_2$	x_9	$N_9 = x_9/\sum x$
	$3\text{CaO}\cdot\text{SiO}_2$	x_{10}	$N_{10} = x_{10}/\sum x$
	$3\text{CaO}\cdot 2\text{SiO}_2$	x_{11}	$N_{11} = x_{11}/\sum x$
	$\text{PbO}\cdot\text{SiO}_2$	x_{12}	$N_{12} = x_{12}/\sum x$
	$2\text{PbO}\cdot\text{SiO}_2$	x_{13}	$N_{13} = x_{13}/\sum x$
	$4\text{PbO}\cdot\text{SiO}_2$	x_{14}	$N_{14} = x_{14}/\sum x$
	$\text{CaO}\cdot\text{Fe}_2\text{O}_3$	x_{15}	$N_{15} = x_{15}/\sum x$
	$2\text{CaO}\cdot\text{Fe}_2\text{O}_3$	x_{16}	$N_{16} = x_{16}/\sum x$
	$\text{CaO}\cdot\text{FeO}\cdot\text{Fe}_2\text{O}_3$	x_{17}	$N_{17} = x_{17}/\sum x$
	$2\text{FeO}\cdot\text{SiO}_2$	x_{18}	$N_{18} = x_{18}/\sum x$
	$\text{CaO}\cdot\text{FeO}\cdot\text{SiO}_2$	x_{19}	$N_{19} = x_{19}/\sum x$
	$\text{ZnO}\cdot\text{SiO}_2$	x_{20}	$N_{20} = x_{20}/\sum x$
	$\text{ZnO}\cdot\text{Fe}_2\text{O}_3$	x_{21}	$N_{21} = x_{21}/\sum x$
	$2\text{ZnO}\cdot\text{SiO}_2$	x_{22}	$N_{22} = x_{22}/\sum x$

In the formula, N_i is the mass action concentration of the structural unit i , x_i is the mole fraction of the structural unit i at equilibrium, and $\sum x$ is the sum of the moles of all structural units in the slag at equilibrium, namely:

$$\sum x = 2 \sum_1^4 x_i + \sum_5^{22} x_i \quad (2)$$

2.3. Determination of the Standard Gibbs Free Energy for the Formation Process of Complex Molecules

All complex molecules in the slag are formed by chemical reactions of simple molecules and ion pairs, so that the equilibrium constant of each complex molecule formation reaction is K_i ; then the mass action concentration N_i of complex molecules can be expressed by K_i and $N_1 \sim N_6$. Each expression of the formula is listed in Table 3.

Table 3. Complex molecule generation reaction equations and their ΔG_i^θ and N_i .

Reaction Equation	ΔG_i^θ (J/mol)	N_i	Ref.
$(\text{Fe}^{2+} + \text{O}^{2-}) + \text{Fe}_2\text{O}_3 = \text{Fe}_3\text{O}_4$	$-45,846 + 10.6 T$	$N_7 = K_1 N_3 N_6$	[18]
$(\text{Ca}^{2+} + \text{O}^{2-}) + \text{SiO}_2 = \text{CaO} \cdot \text{SiO}_2$	$-36,425 - 30.6 T$	$N_8 = K_2 N_4 N_5$	[18]
$2(\text{Ca}^{2+} + \text{O}^{2-}) + \text{SiO}_2 = 2\text{CaO} \cdot \text{SiO}_2$	$-118,905 - 11.3 T$	$N_9 = K_3 N_4^2 N_5$	[18]
$3(\text{Ca}^{2+} + \text{O}^{2-}) + \text{SiO}_2 = 3\text{CaO} \cdot \text{SiO}_2$	$-118,905 - 7.2 T$	$N_{10} = K_4 N_4^3 N_5$	[18]
$3(\text{Ca}^{2+} + \text{O}^{2-}) + 2 \text{SiO}_2 = 3\text{CaO} \cdot 2\text{SiO}_2$	$-236,973 + 9.6 T$	$N_{11} = K_5 N_4^3 N_5^2$	[18]
$(\text{Pb}^{2+} + \text{O}^{2-}) + \text{SiO}_2 = \text{PbO} \cdot \text{SiO}_2$	$-25,121 + 1.3 T$	$N_{12} = K_6 N_1 N_5$	[18]
$2(\text{Pb}^{2+} + \text{O}^{2-}) + \text{SiO}_2 = 2\text{PbO} \cdot \text{SiO}_2$	$-33,494 - 6.7 T$	$N_{13} = K_7 N_1^2 N_5$	[18]
$4(\text{Pb}^{2+} + \text{O}^{2-}) + \text{SiO}_2 = 4\text{PbO} \cdot \text{SiO}_2$	$-67,118 - 615.9T + 99.1 T \ln T - 0.05T^2$	$N_{14} = K_8 N_1^4 N_5$	[11]
$(\text{Ca}^{2+} + \text{O}^{2-}) + \text{Fe}_2\text{O}_3 = \text{CaO} \cdot \text{Fe}_2\text{O}_3$	$-99,218 + 526.6T - 152.83 T \lg T$ (700~1216 °C) $51,672.2 + 205.21 T - 83.46 T \lg T$ (1216~1460 °C)	$N_{15} = K_9 N_4 N_6$	[11]
$2(\text{Ca}^{2+} + \text{O}^{2-}) + \text{Fe}_2\text{O}_3 = 2\text{CaO} \cdot \text{Fe}_2\text{O}_3$	$-53,172 - 2.5 T$	$N_{16} = K_{10} N_4^2 N_6$	[18]
$(\text{Ca}^{2+} + \text{O}^{2-}) + (\text{Fe}^{2+} + \text{O}^{2-}) + \text{Fe}_2\text{O}_3 = \text{CaO} \cdot \text{FeO} \cdot \text{Fe}_2\text{O}_3$	$-14,654 - 27.2 T$	$N_{17} = K_{11} N_3 N_4 N_6$	[18]
$2(\text{Fe}^{2+} + \text{O}^{2-}) + \text{SiO}_2 = 2\text{FeO} \cdot \text{SiO}_2$	$-32,260 + 15.3 T$	$N_{18} = K_{12} N_3^2 N_5$	[18]
$(\text{Fe}^{2+} + \text{O}^{2-}) + \text{SiO}_2 + (\text{Ca}^{2+} + \text{O}^{2-}) = \text{CaO} \cdot \text{FeO} \cdot \text{SiO}_2$	$-72,997 - 29.3 T$	$N_{19} = K_{13} N_3 N_4 N_5$	[18]
$(\text{Zn}^{2+} + \text{O}^{2-}) + \text{SiO}_2 = \text{ZnO} \cdot \text{SiO}_2$	$-1180.89 - 0.2035 T$	$N_{20} = K_{14} N_2 N_5$	[18]
$(\text{Zn}^{2+} + \text{O}^{2-}) + \text{Fe}_2\text{O}_3 = \text{ZnO} \cdot \text{Fe}_2\text{O}_3$	$-1133.88 - 0.2568 T$	$N_{21} = K_{15} N_2 N_6$	[18]
$2(\text{Zn}^{2+} + \text{O}^{2-}) + \text{SiO}_2 = 2\text{ZnO} \cdot \text{SiO}_2$	$-1156.79 - 0.3117 T$	$N_{22} = K_{16} N_2^2 N_5$	[18]

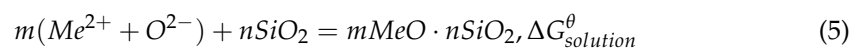
The equilibrium constant K_i in the above chemical reaction is calculated from the standard Gibbs free energy change ΔG_i^θ of the reaction according to Formulas (3) and (4).

$$\Delta G_i^\theta = -RT \ln K_i \quad (3)$$

Namely:

$$K_i = e^{-\frac{\Delta G_i^\theta}{RT}} \quad (4)$$

It is worth mentioning that when calculating the standard Gibbs free energy change ΔG_i^θ of complex molecules composed of ion pairs and simple molecules, the ΔG_i^θ in which the reactants and products are both in solution should be calculated, that is, $\Delta G_{solution}^\theta$. Taking the reaction of metal oxide MeO and SiO_2 to generate $m\text{MeO} \cdot n\text{SiO}_2$ as an example, the reaction formula is as follows:



where m and n are positive integers, $\Delta G_{solution}^\theta$ is the Gibbs free energy change in the reaction when the reactants and products are in solution. However, it is often difficult to obtain thermodynamic data in the dissolved state, and it is relatively easy to obtain thermodynamic data if the reaction is carried out in the solid state. The solid state reaction equation is:



where ΔG_{solid}^θ is the Gibbs free energy change in the reaction when both the reactants and the products are solid.

Dissolving a certain solid phase component into the slag can be divided into two steps. The first step is to melt the component from the solid phase to the liquid phase, and the second step is to dissolve the molten liquid phase into the slag. Thus there are:

$$\Delta G_{solution}^\theta = \Delta G_{solid}^\theta + \Delta_{fus}G_i^\theta + \Delta_{sol}G_i^\theta \quad (7)$$

Among them, $\Delta_{fus}G_i^\theta$ is the standard Gibbs free energy change in the melting process, and $\Delta_{sol}G_i^\theta$ is the standard Gibbs free energy change for dissolving the molten liquid phase into the slag.

Studies have shown that [19], the standard Gibbs free energy change in the component melting process $\Delta_{fus}G_i^\theta$ and the standard Gibbs free energy change in the component dissolving into the slag from the liquid state $\Delta_{sol}G_i^\theta$ are equal in magnitude and opposite in sign, so they can cancel each other out. That is, the standard Gibbs free energy for the formation of complex molecules, whether in solid state or in solution, so $\Delta G_{solid}^\theta = \Delta G_{solution}^\theta$. Therefore, in this paper, the Gibbs free energy change in complex molecular formation reactions is calculated using ΔG_{solid}^θ .

In the studied PbO-ZnO-FeO-Fe₂O₃-SiO₂-CaO six-component slag system, the ΔG_i^θ of partial reactions can be directly obtained by consulting the literature or thermodynamic handbooks. Some that are difficult to obtain directly can be obtained from thermodynamic handbooks or basic data in the literature to make a derivation. The derived formula is shown in Formulas (8)–(10).

$$\Delta H_{298K}^\theta = \sum (n_p \Delta H_{p,298K}^\theta) - \sum (n_r \Delta H_{r,298K}^\theta) \quad (8)$$

$$\Delta \Phi_T = \sum (n_p \Phi_{p,T}) - \sum (n_r \Phi_{r,T}) \quad (9)$$

$$\Delta G_T^\theta = \Delta H_{298K}^\theta - T \Delta \Phi_T \quad (10)$$

In the formula, n_p and n_r are the stoichiometric coefficients of the products and reactants, respectively; $\Delta H_{p,298K}^\theta$ and $\Delta H_{r,298K}^\theta$ are the standard molar formation enthalpy of the products and reactants at 298 K, $\Phi_{p,T}$ and $\Phi_{r,T}$, respectively. The standard Gibbs function of products and reactants at temperature T , ΔH_{298K}^θ is the standard formation enthalpy of the whole reaction at temperature T , and $\Delta \Phi_T$ is the standard Gibbs function of the whole reaction at temperature T . By calculating ΔG_T at different temperatures T , a series of ΔG_T - T data for each reaction can be obtained, and the relationship between ΔG_i and temperature T for each reaction can be obtained through linear fitting, that is, $\Delta G_i = A + B T$.

2.4. Calculation of Mass Action Concentration

We assume that the mole numbers of PbO, ZnO, FeO, CaO, SiO₂, and Fe₂O₃ in the PbO-ZnO-FeO-Fe₂O₃-SiO₂-CaO slag system before equilibrium are n_1 , n_2 , n_3 , n_4 , n_5 , and n_6 , and that for each structural unit 'i' the mole number is x_i , and the mass action concentration is N_i .

According to the ion-molecule coexistence theory, when the equilibrium is reached, the sum of the mass action concentrations of all structural units in the slag is 1, as shown in Formula (11):

$$\sum N_i = 1 \quad (11)$$

According to the law of conservation of mass, the following equations can be obtained, see Equations (12)–(18):

- (1) The total amount of PbO remains unchanged before and after the reaction:

$$n_1 = (0.5N_1 + N_{12} + 2N_{13} + 4N_{14}) \sum x \quad (12)$$

- (2) The amount of total species of ZnO remains unchanged before and after the reaction:

$$n_2 = (0.5N_2 + N_{20} + N_{21} + 2N_{22}) \sum x \quad (13)$$

- (3) The total amount of FeO remains unchanged before and after the reaction:

$$n_3 = (0.5N_3 + N_7 + N_{17} + 2N_{18} + N_{19}) \sum x \quad (14)$$

- (4) The total amount of CaO remains unchanged before and after the reaction:

$$n_4 = (0.5N_4 + N_8 + 2N_9 + 3N_{10} + 3N_{11} + N_{15} + 2N_{16} + N_{17} + N_{19}) \sum x \quad (15)$$

- (5) The total substance amount of SiO₂ remains unchanged before and after the reaction:

$$n_5 = (N_5 + N_8 + N_9 + N_{10} + 2N_{11} + N_{12} + N_{13} + N_{14} + N_{18} + N_{19} + N_{20} + N_{22}) \sum x \quad (16)$$

- (6) The total amount of Fe₂O₃ remains unchanged before and after the reaction:

$$n_6 = (N_6 + N_7 + N_{15} + N_{16} + N_{17} + N_{21}) \sum x \quad (17)$$

Formula (18) can be transformed from Formula (12):

$$\sum x = \frac{n_1}{0.5N_1 + N_{12} + 2N_{13} + 4N_{14}} \quad (18)$$

Bring Formula (13) into Formulas (8)–(12), and eliminate $\sum x$ to obtain Formulas (19)–(23):

$$n_2(0.5N_1 + N_{12} + 2N_{13} + 4N_{14}) - n_1(0.5N_2 + N_{20} + N_{21} + 2N_{22}) = 0 \quad (19)$$

$$n_3(0.5N_1 + N_{12} + 2N_{13} + 4N_{14}) - n_1(0.5N_3 + N_7 + N_{17} + 2N_{18} + N_{19}) = 0 \quad (20)$$

$$n_4(0.5N_1 + N_{12} + 2N_{13} + 4N_{14}) - n_1(0.5N_4 + N_8 + 2N_9 + 3N_{10} + 3N_{11} + N_{15} + 2N_{16} + N_{17} + N_{19}) = 0 \quad (21)$$

$$n_5(0.5N_1 + N_{12} + 2N_{13} + 4N_{14}) - n_1(N_5 + N_8 + N_9 + N_{10} + 2N_{11} + N_{12} + N_{13} + N_{14} + N_{18} + N_{19} + N_{20} + N_{22}) = 0 \quad (22)$$

$$n_6(0.5N_1 + N_{12} + 2N_{13} + 4N_{14}) - n_1(N_6 + N_7 + N_{15} + N_{16} + N_{17} + N_{21}) = 0 \quad (23)$$

Putting the mass action concentrations $N_7 \sim N_{22}$ of each complex molecule in Table 3 into the Formulas (11) and (19)–(23), the Formulas (24)–(29) can be obtained:

$$\begin{aligned} & N_1 + N_2 + N_3 + N_4 + N_5 + N_6 + K_1N_3N_6 + K_2N_4N_5 + K_3N_4^2N_5 + \\ & K_4N_4^3N_5 + K_5N_4^3N_5^2 + K_6N_1N_5 + K_7N_1^2N_5 + K_8N_1^4N_5 + K_9N_4N_6 + \\ & K_{10}N_4^2N_6 + K_{11}N_3N_4N_6 + K_{12}N_3^2N_5 + K_{13}N_3N_4N_5 + K_{14}N_2N_5 + \\ & K_{15}N_2N_6 + K_{16}N_2^2N_5 - 1 = 0 \end{aligned} \quad (24)$$

$$n_2(0.5N_1 + K_6N_1N_5 + 2K_7N_1^2N_5 + 4K_8N_1^4N_5) - n_1(0.5N_2 + K_{14}N_2N_5 + K_{15}N_2N_6 + 2K_{16}N_2^2N_5) = 0 \tag{25}$$

$$n_3(0.5N_1 + K_6N_1N_5 + 2K_7N_1^2N_5 + 4K_8N_1^4N_5) - n_1(0.5N_3 + K_1N_3N_6 + K_{11}N_3N_4N_6 + 2K_{12}N_3^2N_5 + K_{13}N_3N_4N_5) = 0 \tag{26}$$

$$n_4(0.5N_1 + K_6N_1N_5 + 2K_7N_1^2N_5 + 4K_8N_1^4N_5) - n_1(0.5N_4 + K_2N_4N_5 + 2K_3N_4^2N_5 + 3K_4N_4^3N_5 + 3K_5N_4^3N_5^2 + K_9N_4N_6 + 2K_{10}N_4^2N_6 + K_{11}N_3N_4N_6 + K_{13}N_3N_4N_5) = 0 \tag{27}$$

$$n_5(0.5N_1 + K_6N_1N_5 + 2K_7N_1^2N_5 + 4K_8N_1^4N_5) - n_1(N_5 + K_2N_4N_5 + K_3N_4^2N_5 + K_4N_4^3N_5 + 2K_5N_4^3N_5^2 + K_6N_1N_5 + K_7N_1^2N_5 + K_8N_1^4N_5 + K_{12}N_3^2N_5 + K_{13}N_3N_4N_5 + K_{14}N_2N_5 + K_{16}N_2^2N_5) = 0 \tag{28}$$

$$n_6(0.5N_1 + K_6N_1N_5 + 2K_7N_1^2N_5 + 4K_8N_1^4N_5) - n_1(N_6 + K_1N_3N_6 + K_9N_4N_6 + K_{10}N_4^2N_6 + K_{11}N_3N_4N_6 + K_{15}N_2N_6) = 0 \tag{29}$$

Equations (24)–(29) are the activity models of the PbO-ZnO-FeO-Fe₂O₃-SiO₂-CaO slag system. When the composition and temperature of the slag system are determined, $n_1 \sim n_6$ and $K_1 \sim K_{16}$ are known numbers, so there are six equations in the nonlinear equation system composed of Equations (24)–(29), and $N_1 \sim N_6$ are unknown numbers, which can be solved iteratively by least squares programming.

3. Validation of the Activity Model

3.1. Verification of PbO Activity

D. Matsura studied the activity of PbO in the FeO_x-CaO-SiO₂-Na₂O slag system through the slag-gold equilibrium experiment [20]. In order to simplify the slag composition, the literature defines the following:

$$R = \frac{\omega_{CaO}}{\omega_{CaO} + \omega_{SiO_2}} \tag{30}$$

$$Q = \frac{\omega_{FeO_x}}{\omega_{FeO_x} + \omega_{CaO} + \omega_{SiO_2}} \tag{31}$$

In the formula, R is the basicity; Q is the ratio of iron oxides; ω_{FeO_x} , ω_{CaO} , and ω_{SiO_2} are the mass fractions of FeO_x, CaO, and SiO₂, respectively.

When FeO: Fe₂O₃ = 5:1, the mass fraction of PbO is 1%, and the temperature is 1573 K; the comparison between the mass action concentration value of N_{PbO} calculated by the activity model and the experimentally measured activity value is shown in Figure 1:

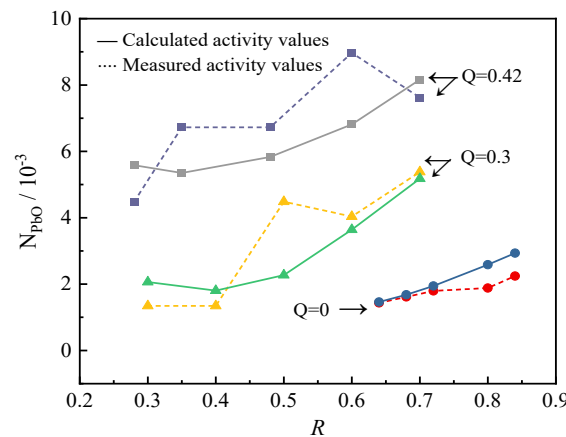


Figure 1. Calculated and measured activity values of PbO.

It can be seen from Figure 1 that the calculated value of the activity model is in good agreement with the experimental measured value, but the deviation from the experimental measured value increases with the increase in Q , which may be caused by the fact that the two types of slag are not completely the same. In the case of $Q \leq 0.42$, the model has good accuracy in calculating the activity of PbO. It can be considered that this model can reflect the structural characteristics of the PbO-ZnO-FeO-Fe₂O₃-SiO₂-CaO slag system.

3.2. Verification of ZnO Activity

Taskinen [21], Sugimoto [22], and Richardson [23] studied the activity of ZnO in the PbO-SiO₂-CaO slag system, respectively, and the comparison results of the experimental measurement value (a_{Exp}) and the model calculation value (N_{Cal}) are as follows in Figure 2.

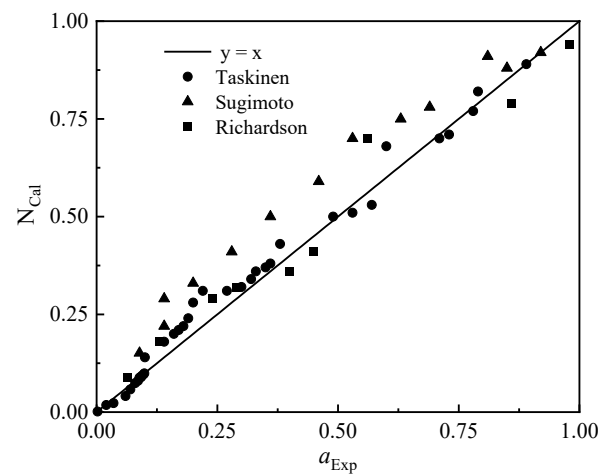


Figure 2. Comparison of ZnO mass action concentration calculations with activity measurements.

It can be seen from Figure 2 that the calculated value of ZnO mass action concentration is in good agreement with the measured value obtained from previous experimental studies, with an average deviation of 18.86%. The calculated mass action concentration is in better agreement with Taskinen's measurement results, and there are some deviations from Sugimoto's measurement results. The area of deviation is that the activity of zinc oxide is between 0.25 and 0.75.

3.3. Verification of FeO Activity

The experimental measurement data of Iwase [24], Fujita [25], and Distin [26] were used to verify the calculated value of FeO activity, and the results are shown in Figure 3.

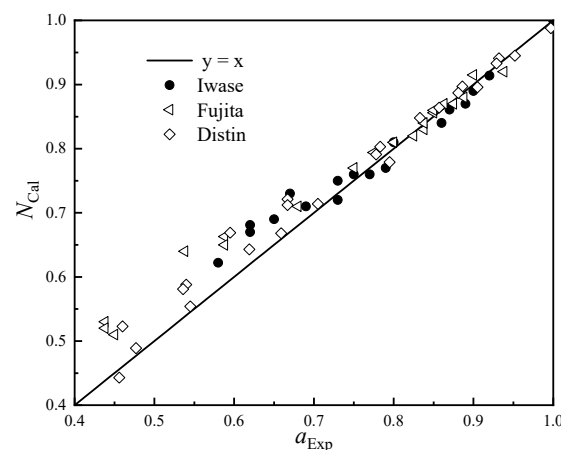


Figure 3. Calculated and measured activity values of FeO.

It can be seen from Figure 3 that the calculated activity of FeO is in good agreement with the measured value as a whole. In the area with high FeO activity, the calculated value is very close to the predicted value, and the area with a large deviation is mainly concentrated in the range of the FeO activity value between 0.4 and 0.7; the calculated value of FeO will be slightly lower than the measured activity value.

4. Results and Discussion

In order to study the influence of temperature and slag type on the activity of each structural unit of high-lead slag, the slag type shown in Table 4 was designed. F/S and C/S are the iron-silicon ratio and the calcium-silicon ratio, respectively, and they will affect the physical properties of the slag.

Table 4. Composition of the designed slag type (mass fraction).

Number	PbO	ZnO	FeO	Fe ₂ O ₃	SiO ₂	CaO	F/S	C/S
1	35.00	5.00	20.00	4.00	24.00	12.00	0.76	0.50
2	40.00	5.00	18.33	3.67	22.00	11.00	0.76	0.50
3	45.00	5.00	16.67	3.33	20.00	10.00	0.76	0.50
4	50.00	5.00	15.00	3.00	18.00	9.00	0.76	0.50
5	55.00	5.00	13.33	2.67	16.00	8.00	0.76	0.50
6	50.00	5.00	10.71	2.14	21.43	10.71	0.46	0.50
7	50.00	5.00	13.04	2.61	19.57	9.78	0.61	0.50
8	50.00	5.00	16.67	3.33	16.67	8.33	0.92	0.50
9	50.00	5.00	18.10	3.62	15.52	7.76	1.07	0.50
10	50.00	5.00	17.86	3.57	21.43	2.14	0.76	0.10
11	50.00	5.00	16.30	3.26	19.57	5.87	0.76	0.30
12	50.00	5.00	13.89	2.78	16.67	11.67	0.76	0.70
13	50.00	5.00	12.93	2.59	15.52	13.97	0.76	0.90
14	50.00	1.00	16.33	3.27	19.60	9.80	0.76	0.50
15	50.00	3.00	15.67	3.13	18.80	9.40	0.76	0.50
16	50.00	7.00	14.33	2.87	17.20	8.60	0.76	0.50
17	50.00	9.00	13.67	2.73	16.40	8.20	0.76	0.50

4.1. Influence of Temperature on the Activity of Each Structural Unit of Slag

We calculated the activity of each structural unit of 4# slag in Table 4 in the temperature range of 1373 K to 1573 K, and the calculation results are shown in Figure 4.

It can be seen from Figure 4 that among all lead-containing compounds, PbO has the largest activity, followed by 2PbO·SiO₂ and PbO·SiO₂, while the activity of 4PbO·SiO₂ is very small, and the maximum activity is in the range of 1373 K~1573 K; The value is also only 4.75×10^{-4} . It shows that the main forms of Pb in high-lead slag are PbO, 2PbO·SiO₂, and PbO·SiO₂. As the temperature increases, the activity of PbO increases continuously, while the activities of 2PbO·SiO₂ and PbO·SiO₂ decrease continuously, indicating that high temperature is beneficial to the decomposition of lead silicate.

The activities of zinc-containing compounds from large to small are ZnO, ZnO·Fe₂O₃, ZnO·SiO₂, and 2ZnO·SiO₂. As the temperature increases from 1373 K to 1573 K, the activity of ZnO decreases from 0.14297 to 0.13507. The activities of ZnO·Fe₂O₃ and ZnO·SiO₂ increased, and the activity of 2ZnO·SiO₂ decreased slightly. It can be considered that the temperature has little effect on the activity of zinc-containing compounds, but the tendency of ZnO to transform into zinc iron spinel and zinc silicate increases when the temperature increases.

Among all iron-containing compounds, FeO has the highest activity. In the studied temperature range, its activity remains above 0.27 and increases to 0.2834 at a temperature of 1573 K. It is the largest activity structural unit of the slag type in the range of 1373~1573 K. It is worth noting that with the increase in temperature, the activity of FeO and Fe₂O₃ will increase slightly, and the activity of Fe₃O₄ will decrease slightly. The trend of combining FeO and Fe₂O₃ to form Fe₃O₄ is weakened at high temperature. As the temperature

increases, the activities of $\text{CaO}\cdot\text{FeO}\cdot\text{Fe}_2\text{O}_3$, $\text{CaO}\cdot\text{Fe}_2\text{O}_3$, and $2\text{CaO}\cdot\text{Fe}_2\text{O}_3$ ferrite calcium salts all increase, and the activities of $\text{CaO}\cdot\text{FeO}\cdot\text{SiO}_2$ and $2\text{FeO}\cdot\text{SiO}_2$ decrease, which also shows that when the temperature increases, part of Fe combined with SiO_2 will be combined with CaO instead.

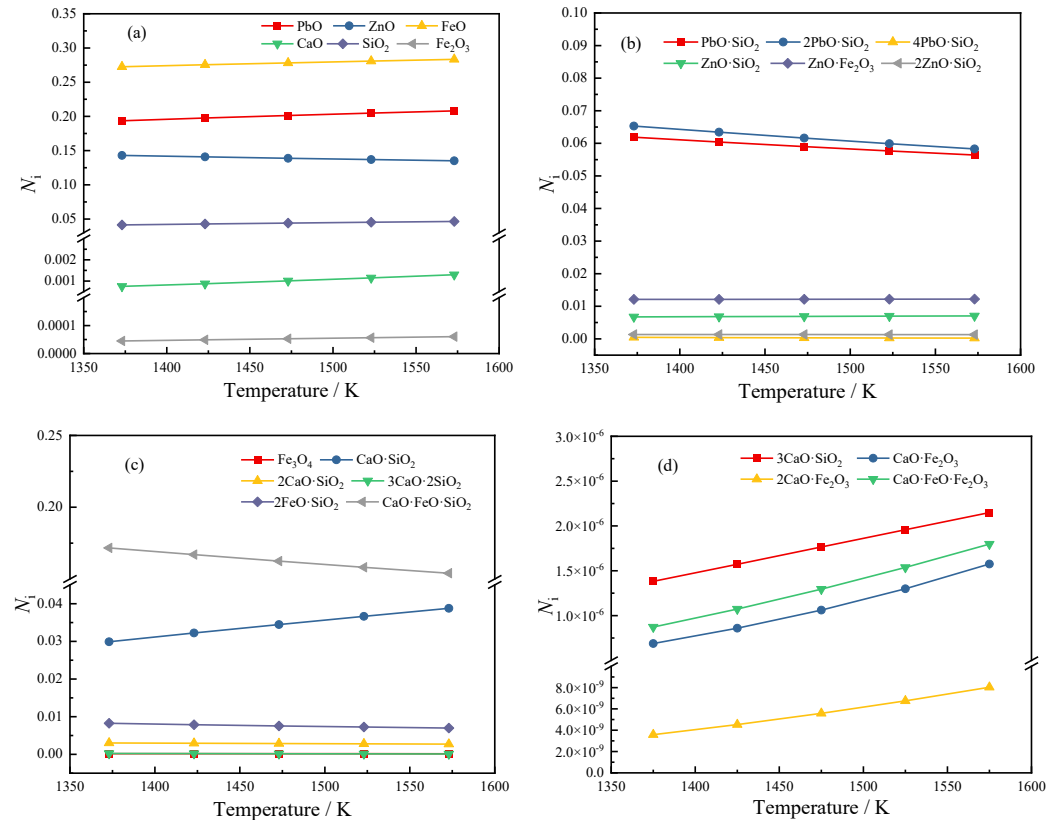


Figure 4. Activity of each structural unit at different temperatures: (a) initial component; (b) lead-zinc compound; (c) some complex molecules of iron-silicon-calcium salt; (d) some complex molecules with extremely low activity.

Unlike other initial components such as PbO , ZnO , FeO , etc., the activity of free CaO in the slag is very small, indicating that most of CaO will react with SiO_2 and iron oxides in the slag to form various complex molecules. Among them, $\text{CaO}\cdot\text{FeO}\cdot\text{SiO}_2$ has the largest activity. Among the complex molecules formed by the combination of CaO and SiO_2 , the activity of $\text{CaO}\cdot\text{SiO}_2$ is much greater than that of $2\text{CaO}\cdot\text{SiO}_2$, $3\text{CaO}\cdot 2\text{SiO}_2$, and $3\text{CaO}\cdot\text{SiO}_2$. The reason may be that the CaO content is not much or the temperature is not high enough. When the temperature rises, it can be found that the activity of $3\text{CaO}\cdot\text{SiO}_2$ increases significantly, indicating that the rise in temperature is beneficial to its formation.

4.2. Effect of Slag Composition Variation on Activity of Pb-Zn Compounds

In order to explore the influence of slag composition changes on the activity of lead-zinc compounds, the mass concentration of each structural unit of 1#~17# slag at 1473 K was calculated, and the results are shown in Figure 5.

It can be seen from Figure 5a that when the mass fraction of PbO is 35%, the activity of PbO is only 0.1056, and when the mass fraction of PbO is 55%, the activity is 0.2498. With the increase in the mass fraction of PbO , the activity of PbO increased rapidly, and the increasing trend became faster and faster. At the same time, the activity of $\text{PbO}\cdot\text{SiO}_2$ decreases and the activity of $2\text{PbO}\cdot\text{SiO}_2$ increases. It shows that when the mass fraction of PbO is low, it mainly combines with SiO_2 to form $\text{PbO}\cdot\text{SiO}_2$, and when the mass fraction of PbO increases, part of PbO will continue to combine with $\text{PbO}\cdot\text{SiO}_2$ to form $2\text{PbO}\cdot\text{SiO}_2$. The activity of ZnO will also increase with the increase in the mass fraction of PbO , which

may be caused by the decrease in the amount of ZnO combined with SiO₂ due to the increase in PbO.

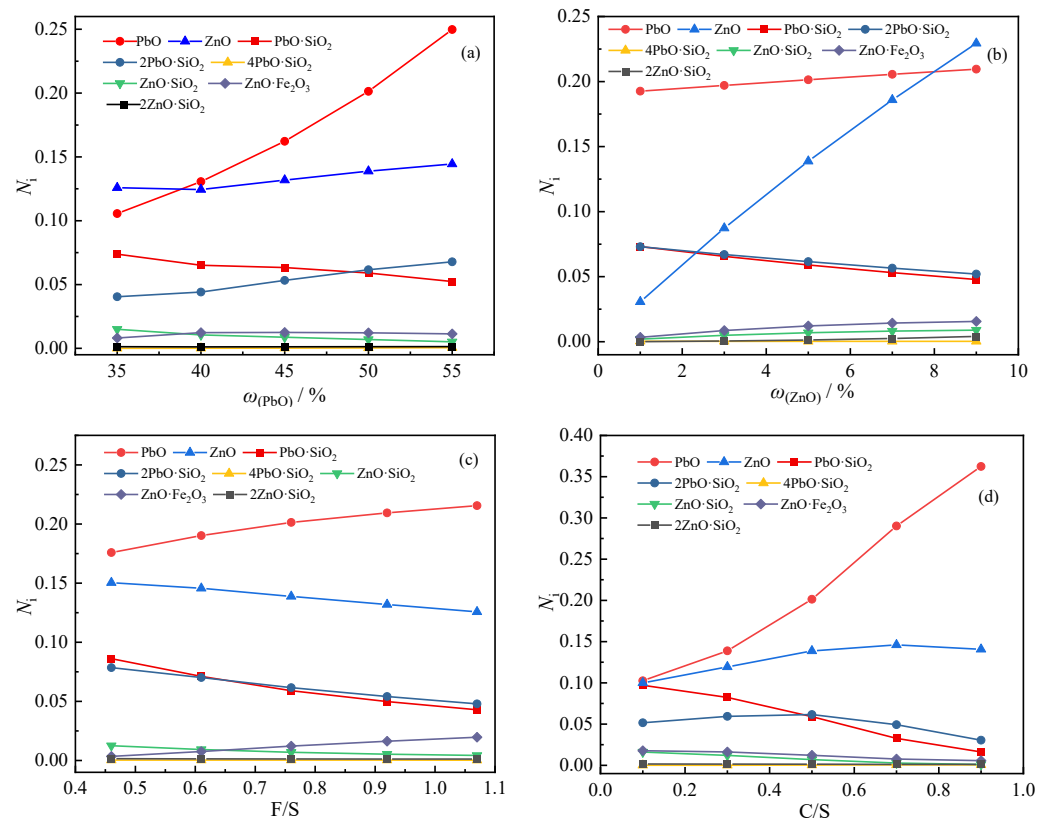


Figure 5. Activity of lead and zinc compounds in slags with different compositions: (a) mass fraction of lead; (b) mass fraction of zinc; (c) iron-silicon ratio; (d) calcium-silicon ratio.

As shown in Figure 5b, when the mass fraction of ZnO increases, in addition to the activity of various zinc-containing compounds increasing, the activity of PbO will also increase, while the activities of PbO·SiO₂ and 2PbO·SiO₂ will decrease; it shows that the increase in ZnO will decompose part of PbO·SiO₂ and 2PbO·SiO₂. It can be seen that the activity and increase rate of ZnO are much greater than those of other zinc-containing compounds, indicating that zinc in this slag system mainly exists in the form of ZnO.

According to Figure 5c, the increase in the iron-silicon ratio will lead to an increase in the activity of PbO, and the activity of PbO·SiO₂ and 2PbO·SiO₂ will decrease, which is also caused by the reduction in SiO₂ that can be combined with PbO. At the same time, the activity of ZnO and ZnO·SiO₂ will also decrease, while the activity of ZnO·Fe₂O₃ will increase significantly. When the iron-silicon ratio increases from 0.46 to 1.07, the activity of ZnO·Fe₂O₃ increases from 0.00350 to 0.01965, indicating that when the iron content increases, a part of ZnO will react with it to form the zinc-iron spinel phase.

It can be seen from Figure 5d that the increase in the calcium-silicon ratio has a great influence on the activity of lead-containing compounds. When the calcium-silicon ratio increases to 0.9, the activity of PbO increases sharply to 0.362, while the activity of PbO·SiO₂ will also decrease rapidly, and the activity of 2PbO·SiO₂ will also decrease after the calcium-silicon ratio is greater than 0.5. The possible reason is that the binding ability of CaO to SiO₂ is stronger than that of PbO. Similar to PbO, the activity of ZnO also increases with the increase in the calcium-silicon ratio, but its increasing trend gradually tends to be flat, probably because the ZnO·SiO₂ and 2ZnO·SiO₂ in the slag are less and less at this time. ZnO almost all exist in free form.

4.3. The Change in Calcium Silicate Activity When Calcium-Silicon Ratio Increases

It can be seen from the previous research that the change in the calcium-silicon ratio has a great influence on the composition and properties of the slag, so it is necessary to study the activity of calcium-silicate in the slag when the calcium-silicon ratio changes. When the calcium-silicon ratio increases from 0.1 to 0.9, the calculated activity values of the binary calcium silicate in the slag are shown in Figure 6.

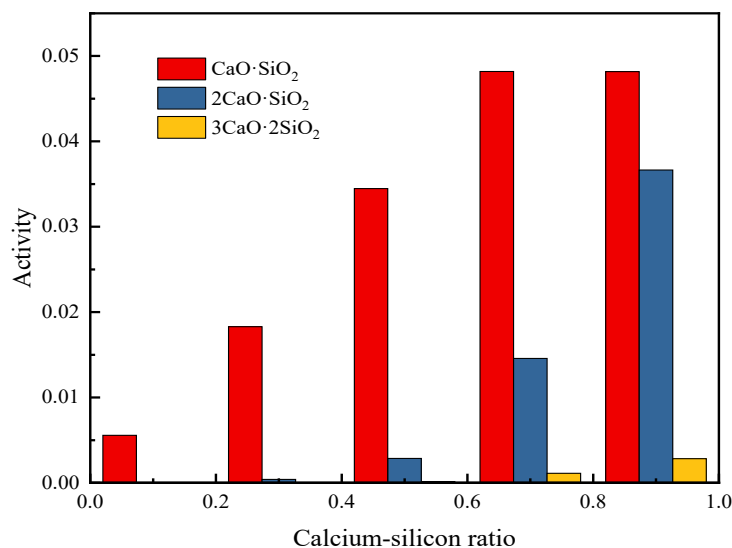


Figure 6. Activity of binary binding products of CaO and SiO₂ at different CaO/SiO₂.

Figure 6 shows the activities of CaO·SiO₂, 2CaO·SiO₂, and 3CaO·2SiO₂ at different calcium-silicon ratios at a temperature of 1473 K (the activity value of 3CaO·SiO₂ is not shown in the figure). It can be seen that when the calcium-silicon ratio is low, CaO and SiO₂ are mainly combined into CaO·SiO₂, and as the calcium-silicon ratio increases, 2CaO·SiO₂ and 3CaO·2SiO₂ with higher melting points appear, and the activity continues to increase. When the calcium-silicon ratio is 0.5, the activity of 2CaO·SiO₂ is still relatively small, but when the calcium-silicon ratio increases to 0.7, the activity of 2CaO·SiO₂ increases by 6.2 times. In order to reduce the viscosity of the slag, the calcium-silicon ratio should be around 0.5.

5. Conclusions

The calculated results of the activity model are in good agreement with the experimental measurements, which can better reflect the real structural characteristics of the slag. The activity of each structural unit is greatly affected by the composition of the slag, but less affected by temperature. High temperature is conducive to the decomposition of lead silicate and the formation of calcium-containing compounds, but the activity of ZnO will decrease, and the tendency of FeO and Fe₂O₃ to form Fe₃O₄ will be weakened. When the mass fraction of PbO increases, the main reaction is to combine with PbO·SiO₂ to form 2PbO·SiO₂. Increasing the mass fraction of ZnO and CaO is beneficial to the decomposition of lead silicate and an increase in PbO activity. When the iron-silicon ratio increases, it will promote the decomposition of lead silicate and the formation of ZnO·Fe₂O₃, so the activity of PbO will increase and the activity of ZnO will decrease. When the calcium-silicon ratio is low, the binary combination product of CaO and SiO₂ is mainly CaO·SiO₂, and when the calcium-silicon ratio rises above 0.5, the activities of 2CaO·SiO₂ and 3CaO·2SiO₂ will increase rapidly.

Author Contributions: Conceptualization, J.S. and W.X.; Methodology, J.S.; Software, J.S.; Validation, J.S.; Formal analysis, W.X.; Investigation, W.X.; Resources, W.X.; Writing—original draft, J.S.; Writing—review & editing, W.X.; Visualization, L.N.; Supervision, L.N.; Project administra-

tion, L.N.; Funding acquisition, L.N. All authors have read and agreed to the published version of the manuscript.

Funding: The authors are grateful for financial support from the National Key R&D Program of China (No. 2019YFC1907301) and National Natural Science Foundation of China (No. 51874094).

Data Availability Statement: All data generated or analyzed during this study are included in this article.

Conflicts of Interest: On behalf of all authors, the corresponding author states that there are no conflict of interest.

References

1. Yang, J.; Li, X.; Xiong, Z.; Wang, M.; Liu, Q. Environmental pollution effect analysis of lead compounds in China based on life cycle. *Int. J. Environ. Res. Public Health* **2020**, *17*, 2184. [[CrossRef](#)] [[PubMed](#)]
2. Agrawal, A.; Sahu, K.K.; Pandey, B.D. Solid waste management in non-ferrous industries in India. *Resour. Conserv. Recycl.* **2004**, *42*, 99–120. [[CrossRef](#)]
3. Liu, S.; Fruehan, R.J.; Morales, A.; Ozturk, B. Measurement of FeO activity and solubility of MgO in smelting slags. *Metall. Mater. Trans. B* **2001**, *32*, 31–36. [[CrossRef](#)]
4. Espejo, V.; Iwase, M. A thermodynamic study of the system $\text{CaO} + \text{Al}_2\text{O}_3 + \text{Fe}_x\text{O}$ at 1673 K. *Metall. Mater. Trans. B* **1995**, *26*, 257–264. [[CrossRef](#)]
5. Sun, S.; Jahanshahi, S. Redox equilibria and kinetics of gas-slag reactions. *Metall. Mater. Trans. B* **2000**, *31*, 937–943. [[CrossRef](#)]
6. Lin, P.L.; Pelton, A.D. A structural model for binary silicate systems. *Metall. Trans. B* **1979**, *10*, 667–675. [[CrossRef](#)]
7. Sastri, P.; Lahiri, A.K. Applicability of central atoms models to binary silicate and aluminate melts. *Metall. Trans. B* **1985**, *16*, 325–331. [[CrossRef](#)]
8. Tijssens, E.; Viaene, W.A.; Geerlings, P. The ionic model: Extension to spatial charge distributions, derivation of an interaction potential for silica polymorphs. *Phys. Chem. Miner.* **1995**, *22*, 186–199. [[CrossRef](#)]
9. Ping Tao, D. Prediction of activities of three components in the ternary molten slag CaO-FeO-SiO_2 by the molecular interaction volume model. *Metall. Mater. Trans. B* **2006**, *37*, 1091–1097. [[CrossRef](#)]
10. Mao, L.; Wu, Y.; Hu, L.; Huang, Q.; Dai, Z.; Zhang, W. Activity calculation and phase transformation prediction for heavy metals with slag activity calculation model during using electroplating sludge in production of bricks. *J. Environ. Chem. Eng.* **2019**, *7*, 103242. [[CrossRef](#)]
11. Wang, J.; Wen, X.; Zhang, C. Thermodynamic model of lead oxide activity in $\text{PbO-CaO-SiO}_2\text{-FeO-Fe}_2\text{O}_3$ slag system. *Trans. Nonferrous Met. Soc. China* **2015**, *25*, 1633–1639. [[CrossRef](#)]
12. Kudo, M.; Jak, E.; Hayes, P.; Yamaguchi, K.; Takeda, Y. Lead solubility in FeO-x-CaO-SiO_2 slags at iron saturation. *Metall. Mater. Trans. B* **2000**, *31*, 15–24. [[CrossRef](#)]
13. Shi, C.; Yang, X.; Jiao, J.; Li, C.; Guo, H. A sulphide capacity prediction model of $\text{CaO-SiO}_2\text{-MgO-Al}_2\text{O}_3$ ironmaking slags based on the ion and molecule coexistence theory. *ISIJ Int.* **2010**, *50*, 1362–1372. [[CrossRef](#)]
14. Yang, X.M.; Shi, C.B.; Zhang, M.; Zhang, J. A Thermodynamic Model for Prediction of Iron Oxide Activity in Some FeO-Containing Slag Systems. *Steel Res. Int.* **2012**, *83*, 244–258. [[CrossRef](#)]
15. Yang, X.; Zhang, M.; Shi, C.; Chai, G.; Zhang, J. A sulfide capacity prediction model of $\text{CaO-SiO}_2\text{-MgO-FeO-MnO-Al}_2\text{O}_3$ slags during the LF refining process based on the ion and molecule coexistence theory. *Metall. Mater. Trans. B* **2012**, *43*, 241–266. [[CrossRef](#)]
16. Jak, E.; Zhao, B.; Hayes, P.C.; Liu, N. Experimental study of phase equilibria in the system PbO-ZnO-SiO_2 . *Metall. Mater. Trans. B* **1999**, *30*, 21–27. [[CrossRef](#)]
17. Zhang, J. *Computational Thermodynamics of Metallurgical Melts and Solutions*; Metallurgical Industry Press: Beijing, China, 2007; p. 562.
18. Ye, D. *Handbook of Practical Inorganic Thermodynamic Data*; Metallurgical Industry Press: Beijing, China, 1980; p. 1120.
19. Yang, X.; Shi, C.; Zhang, M.; Duan, J.; Zhang, J. A thermodynamic model of phosphate capacity for $\text{CaO-SiO}_2\text{-MgO-FeO-Fe}_2\text{O}_3\text{-MnO-Al}_2\text{O}_3\text{-P}_2\text{O}_5$ slags equilibrated with molten steel during a top–bottom combined blown converter steelmaking process based on the ion and molecule coexistence theory. *Metall. Mater. Trans. B* **2011**, *42*, 951–977. [[CrossRef](#)]
20. Matura, D.; Ueda, S.; Yamaguchi, K. Lead Solubility in $\text{FeO}_x\text{-CaO-SiO}_2\text{-NaO}0.5$ and $\text{FeO}_x\text{-CaO-SiO}_2\text{-CrO}1.5$ Slags under Iron Saturation at 1573 K. *High Temp. Mater. Process.* **2011**, *30*, 441–446. [[CrossRef](#)]
21. Taskinen, P.; Taskinen, A.; Holappa, L.E. Solution Thermodynamics of PbO-CaO-SiO_2 Melts. *Can. Metall. Q.* **1982**, *21*, 163–169. [[CrossRef](#)]
22. Sugimoto, E.; Kozuka, Z. Effect of CaO , Al_2O_3 , MgO and ZnO on the Activity of PbO in the Molten PbO-SiO_2 System. *Trans. Jpn. Inst. Met.* **1978**, *19*, 275–280. [[CrossRef](#)]
23. Richardson, F.D.; Pillay, T. Lead oxide in molten slags. *Trans. Inst. Min. Metall.* **1957**, *66*, 309–329.
24. Iwase, M.; Ogura, T.; Tsujino, R. Automatic FeO activity determinator for slag control. *Steel Res.* **1994**, *65*, 90–93. [[CrossRef](#)]

25. Fujita, H.; Iritani, Y.; Maruhashi, S. Activities in the Iron-Oxide Lime Slag. *Tetsu-Hagane* **1968**, *54*, 359–370. [[CrossRef](#)] [[PubMed](#)]
26. Distin, P.A.; Whiteway, S.G.; Masson, C.R. Thermodynamics and constitution of ferrous silicate melts. *Can. Metall. Quart.* **1971**, *10*, 73–78. [[CrossRef](#)]

Disclaimer/Publisher’s Note: The statements, opinions and data contained in all publications are solely those of the individual author(s) and contributor(s) and not of MDPI and/or the editor(s). MDPI and/or the editor(s) disclaim responsibility for any injury to people or property resulting from any ideas, methods, instructions or products referred to in the content.